J. of Basic Sciences, Cheju Nat'l Univ.
17(2), 127~137, 2004

기초과학연구 제주대학교
17(2), 127~137, 2004

Synthesis and Characterization of Binuclear Ni(II) Complex with 22-Membered Phenol-Based N_4O_2 Compartmental Macrocyclic Ligand

Chung-Hun Han, Ki-Ju Kim, Chang-Sik Hyun, and Jong-Chul Byun

Department of Chemistry, College of Natural Science, Cheju National University

Abstract. A dinuclear nickel(II) complex with [2+2] symmetrical N_4O_2 compartmental macrocyclic ligand {H_2[22]-HMTADO : 5.5.11.17.17.23-hexamethyl-3.7.15.19-tetraazatricyclo[19.3.1.1^{9,13}]hexacosa-1(25).2.7.9.11.13(26).14.19.21.23-decane-25.26-diol} containing bridging phenolic oxygen atoms was synthesized by condensation, in the nicke(II) ions, of 2.6-diformyl-*p*-cresol and 2.2-dimethyl-1.3-propandiamine. Single-crystal X-ray diffraction studies are reported for $[Ni_2([22]\text{-}HMTADO)(H_2O)_4](ClO_4)_2 \cdot 3H_2O$. $[Ni_2([22]\text{-}HMTADO)(H_2O)_4](ClO_4)_2 \cdot 3H_2O$ crystallized in the monoclinic system, space group P2(1)/c, a = 9.4152(6) Å, b = 22.2913(13) Å, c = 18.2102(11) Å, α = 90°, β = 95.2790(10)°, γ = 90°, and Z = 4. Octahedral two nickel ions stereochemistries are observed with axially coordinated water molecules. The structure of the complexes has been elucidated by elemental analysis, molar conductance, mass, IR, and electronic studies. The complexes exhibit high thermal stability and the macrocyclic entity remains unchanged up to 380℃.

Key words : nickel complexes, macrocyclic ligand complexes

I. Introduction

Polyamines are essential for life.[1] As a result, many studies have targeted polyamine as a potential site for chemotherapeutic intervention.[2] Macrocyclic complexes with a tetraaza-macrocyclic ligand (e.g., cyclen, cyclam, and bicyclam) and their derivatives have found utility in antitumor[3-6] and anti-HIV[7, 8] applications.

Over the past decade, many studies have been focused upon metal complexes of cyclic triamines which cleaving carboxyester[9], phos-phoester[10-14], RNA[15, 16], DNA[17, 18], dipeptides and proteins[19]. To our knowledge, few papers published for the cytotoxic properties and the *in vivo* antitumor effects of triazacyclic polyamines metal complexes[20, 21].

The application of designer compartmental ligands to the study of dinuclear metal complexes first occurred in the early 1970s and the term binucleating ligand was introduced by Robson[22] for polydentate chelating ligands that are capable of simultaneously binding two metal ions in close proximity. If the metal ions used are of the same type then the term homondinuclear is used and if the two metal ions are different then the complex is termed heterodinuclear.

One interest in such bimetallic complexes lies in the area of magnetochemistry. Studies on the magnetic properties of homo- and hetero-dinuclear complexes have significantly helped in advancing

our understanding of spin-exchange mechanisms, relating them to the geometries and to the ground state electronic configurations of the constituting metal ions, and to the nature of the bridging group[23]. A second area of interest is bioinorganic chemistry where dinuclear complexes can serve as synthetic analogs for bimetallobiosites and so give insight into the significance of the bimetallic cores present therein[24]. This is very topical with the recent recognition of the heterodinuclear cores at the metallobiosites in purple acid phosphatase (FeZn)[25], human calcineurin (FeZn)[26] and human protein phosphatase 1 (MnFe)[27] stimulating a search for model complexes of unsymmetrical ligands which can bind two dissimilar metal ions in close proximity[28].

Various types of compartmental ligands in -cluding the end-off type, the side-off type and the macrocyclic type have been developed[29-32]. The macrocyclic Schiff bases (1), derived from the [2+2] condensation of a 2,6-diacyl-substituted phenol and a diamine, form a unique family of compartmental ligands.

Many modifications can be made to the basic structure such as the provision of different lateral

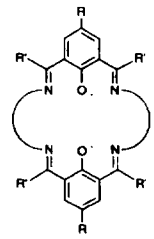

1

chains, the introduction of an additional donor atom on one lateral chain, and partial or full saturation at the azomethine linkages. For the macrocycles which have been reduced at the azomethine groups, a potentially donating auxiliary can be introduced at the aminic nitrogen as a pendant arm. Unsymmetrical modifications of the macrocycles are of importance for providing discrete heterodinuclear core complexes. The present review is concerned with heterodinuclear metal complexes derived from symmetrical and unsymmetrical phenol-based compartmental ligands of this family.

Recent attention is directed to the organization of three or more metal centers in predetermined arrays using polynucleating macrocyclic ligands. For example, tetranuclear Ni(II) and Zn(II)[33] and

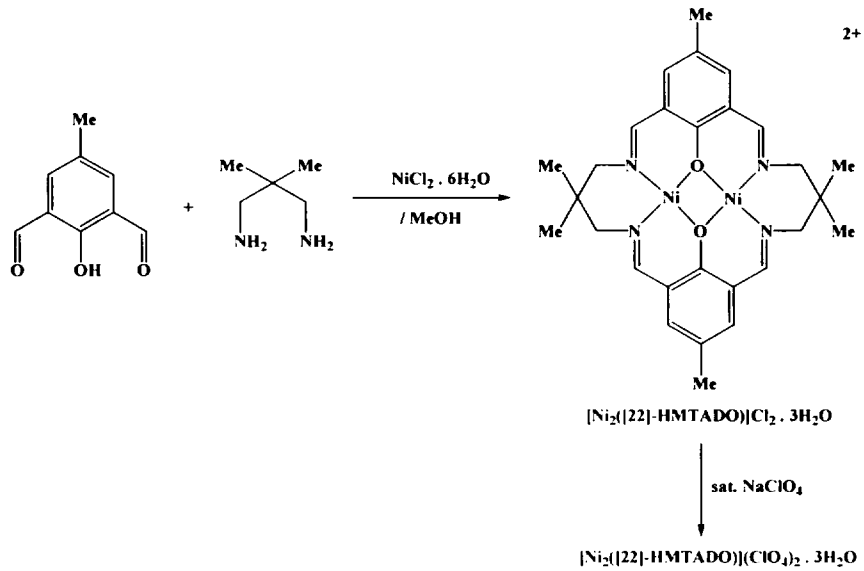

Scheme 1. Synthesis of the binuclear Ni(II) complexes of phenol-based macrocyclic ligand (H_2[22]-HMTADO).

hexanuclear Cu(II)[34] complexes have been obtained by the [2 + 2] or [3 + 3] condensation between 2.6-diformyl-4-methylphenol and 2.6-bis(aminomethyl)-4-methyl-phenol in the presence of a metal ion. Furthermore, the [2 + 2] condensation product between 2.6-diformyl-4-methylphenol and 1.5-diamino-3-pentanol has been used to produce tetra-, octa- and dodecanuclear Cu(II) complexes.[33, 35, 36]

This work performs synthesis and physicochemical characterization of dinuclear nickel(II) complex with [2+2] symmetrical N_4O_2 compartmental macrocyclic ligand {H_2[22]-HMTADO : 5.5.11.17.17.23-hexamethyl-3.7.15.19-tetraazatricyclo[19.3.1.1^{9,13}]hexacosa-1(25).2.7.9.11.13(26).14.19.21.23-decane-25.26-diol} containing bridging phenolic oxygen atoms was synthesized by condensation in the nicke(II) ions of 2.6-diformyl-*p*-cresol and 2.2-dimethyl-1.3-propandiamine (Scheme 1). Single-crystal X-ray diffraction studies are reported for [Ni_2([22]-HMTADO)$(H_2O)_4$]$(ClO_4)_2 \cdot 3H_2O$.

II. Experimental

1. Chemicals and Physical Measurements

All chemicals were commercial analytical reagents and were used without further purification. For the spectroscopic and physical measurements, organic solvents were dried and purified according to the literature methods[37]. Nanopure quality water was used throughout this work. Microanalyses of C, H, and N was carried out using LECO CHN-900 analyzer. Conductance measurement of the complex was performed at 25±1℃ using an ORION 162 conductivity temperature meter. IR spectrum was recorded with a Bruker FSS66 FT-IR spectrometer in the range 4000-370 cm^{-1} using KBr pellets. Electronic absorption spectrum was measured at 25℃ on a UV-3150 UV-VIS-NIR Spectrophotometer (SHIMADZU). FAB-mass spectrum was obtained on a JEOL JMS-700 Mass Spectrometer using argon (6 kV, 10 mA) as the FAB gas. The accelerating voltage was 10 kV andglycerol was used as the matrix. The mass spectrometer was operated in positive ion mode and mass spectrum was calibrated by Alkali-CsI positive.

2. Preparations

1) 2.6-diformyl-*p*-cresol.

The synthesis of 2.6-diformyl-*p*-cresol was prepared according to the literature methods previously reported.[38, 39]

2) [Ni_2([22]-HMTADO)]$Cl_2 \cdot 3H_2O$ (1).

Nickel chloride hexahydrate (4.80 g), 2.6-diformyl-*p*-cresol (1.64 g), and 2-dimethyl-1.3-propandiamine (1.03 g) were heated under reflux in methanol (150 mL) for 4 h. The solution was cooled to room temperature and the pale green product was filtered, thoroughly washed with ice-cold methanol, dried under vacuum over anhydrouse calcium chloride. Yield 1.462 g (42%). *Anal.* Calc. (%) for $Ni_2(C_{28}H_{34}N_4O_2)Cl_2 \cdot (H_2O)_3$: C, 47.98 : H, 5.75 : N, 7.99. Found (%) : C, 47.99 : H, 5.02 : N, 7.66. Solubility : water, DMSO, DMF, hot acetonitrile, hot acetone, chloroform. Λ_M (water) : 205 $ohm^{-1}cm^2mol^{-1}$.

3) [Ni_2([22]-HMTADO)]$(ClO_4)_2 \cdot 3H_2O$ (2).

A brown solution of (1) (0.701 g) in hot water (100 mL) was added dropwise a saturated aqueous sodium perchlorate solution (4 mL) with stirring and the solution was refluxed for 2 h. Then the solution stored in a refrigerator until the pale brown crystals formed on the upper part of the flask. The product was filtered off, thoroughly washed with ice-cold water, and dried in vacuo. Yield 0.408 g (49%). *Anal.* Calc. (%) for Ni$_2$($C_{28}H_{34}N_4O_2$) $\cdot (ClO_4)_2 \cdot (H_2O)_3$: C, 40.57 : H, 4.86 : N, 6.76. Found (%) : C, 40.95 : H, 4.57 : N,

6.75. Solubility : methanol. DMSO. DMF. acetonitrile. acetone. Λ_M (methanol) : 170 $ohm^{-1}cm^2mol^{-1}$.

Table 1. Crystal data and structure refinement for $[Ni_2([22]\text{-HMTADO})(H_2O)_4](ClO_4)_2 \cdot 3H_2O$

Empirical formula	$C_{28}H_{48}Cl_2N_4Ni_2O_{17}$
Formula weight	901.02
Temperature	446(2) K
Wavelength	0.71073 Å
Crystal system	Monoclinic
Space group	P2(1)/c
Unit cell dimensions	a = 9.4152(6) Å α = 90°
	b = 22.2913(13) Å β = 95.2790(10)°
	c = 18.2102(11) Å γ = 90°
Volume	3805.7(4) $Å^3$
Z	4
Density (calculated)	1.573 g/cm^3
Absorption coefficient	1.206 mm^{-1}
F(000)	1880
Crystal size	0.45 x 0.35 x 0.15 mm^3
Theta range for data collection	1.83 to 28.27°.
Index ranges	$-12 \le h \le 11$, $-28 \le k \le 26$, $-21 \le l \le 23$
Reflections collected	24087
Independent reflections	8863 [R(int) = 0.0659]
Completeness to theta = 28.27°	93.8 %
Absorption correction	None
Refinement method	Full-matrix least-squares on F^2
Goodness-of-fit on F^2	1.046
R indices [I>2sigma(I)]	R_1 = 0.0328, wR_2 = 0.0888
R indices (all data)	R_1 = 0.0427, wR_2 = 0.0952

$R = \sum||F_o|-|F_c||/\sum|F_o|$, $R_w = [\sum w(F_o^2 - F_c^2)^2/\sum w(F_o^2)^2]^{1/2}$

$w = 1/[\sigma^2(F_o^2) + (0.0451P)^2 + 1.7091P]$

where $P = (F_o^2 + 2F_c^2)/3$.

3. Crystallogrraphy of the $[Ni_2([22]\text{-HMTADO})(H_2O)_4](ClO_4)_2 \cdot 3H_2O$.

Crystallization from water formed $[Ni_2([22]\text{-HMTADO})(H_2O)_4](ClO_4)_2 \cdot 3H_2O$ as good crystals suitable for X-ray crystallography. The pale brown crystal of $[Ni_2([22]\text{-HMTADO})(H_2O)_4](ClO_4)_2 \cdot 3H_2O$ was attached to glass fibers and mounted on a Bruker SMART diffractometer equipped with a graphite mono-chromated Mo Kα (= 0.71073 Å) radiation. operating at 50 kV and 30 mA and a CCD detector : 45 frames of two-dimensional diffraction images were collected and processed to obtain the cell parameters and orientation matrix. The crystallographic data. conditions for the collection of intensity data. and some features of the structure refinements are listed in Table 1. and atomic coordinates were given in Table 2. The intensity data were corrected for Lorentz and polarization effects. Absorption correction was not made during processing. Of the 24087 unique reflections measured. 8863 reflections in the range $1.83° \le 2\theta \le 28.27°$ were considered to be observed($I > 2\sigma(I)$) and were used in subsequent structure analysis. The program SAINTPLUS[40] was used for integration of the diffraction profiles. The structures were solved by direct methods using the SHELXS program of the SHELXTL package[41] and refined by full matrix least squares against F^2 for all data using SHELXL. All non-H atoms were refined with anisotropic displacement parameters (Table 3). Hydrogen atoms were placed in idealized positions [U_{iso} = 1.2U_{eq}(parent atom)].

III. Results and discussion

1. Description of the structure

An ORTEP view of $[Ni_2([22]\text{-HMTADO})(H_2O)_4](ClO_4)_2 \cdot 3H_2O$ is shown in Fig. 1. and bond distances and angles are summarized in Table 4 and 5. The crystal structure of this complex is composed of dinuclear cation of the indicated formula and noninteracting chloride anions. These results are backed up by the molar conductivity (Λ_M = 170 $ohm^{-1}cm^2mol^{-1}$) which agreed with assignment of the structure as $[Ni_2([22]\text{-HMTADO})(H_2O)_4](ClO_4)_2 \cdot 3H_2O$. The dimeric cation. $[Ni_2([22]\text{-HMTADO})(H_2O)_4]^{2+}$ shows two octahedral environment.

Table 2. Atomic coordinates ($x10^4$) and equivalent isotropic displacement parameters ($Å^2x\ 10^3$) for $[Ni_2([22]\text{-HMTADO})(H_2O)_4](ClO_4)_2 \cdot 3H_2O$

	x	y	z	U(eq)
Ni(1)	1797(1)	6817(1)	8813(1)	17(1)
Ni(2)	-691(1)	7442(1)	9488(1)	17(1)
Cl(1)	1276(1)	5720(1)	6193(1)	28(1)
O(3)	2415(3)	5299(1)	6206(2)	73(1)
O(4)	185(2)	5563(1)	5646(1)	55(1)
O(5)	707(2)	5714(1)	6898(1)	49(1)
O(6)	1803(2)	6309(1)	6054(1)	47(1)
Cl(2)	4328(1)	8727(1)	6524(1)	25(1)
O(7)	4578(2)	9265(1)	6943(1)	50(1)
O(8)	2905(2)	8520(1)	6568(1)	50(1)
O(9)	5307(2)	8266(1)	6814(1)	38(1)
O(10)	4553(2)	8837(1)	5765(1)	34(1)
O(1W)	3001(2)	7031(1)	9825(1)	21(1)
O(2W)	428(2)	6723(1)	7799(1)	24(1)
O(3W)	856(2)	7595(1)	10470(1)	21(1)
O(4W)	-1935(2)	7259(1)	8483(1)	24(1)
O(1)	124(1)	6606(1)	9395(1)	18(1)
O(2)	922(2)	7636(1)	8874(1)	19(1)
N(1)	2461(2)	5962(1)	8864(1)	20(1)
N(2)	-2128(2)	7129(1)	10131(1)	19(1)
N(3)	-1305(2)	8303(1)	9496(1)	20(1)
N(4)	3384(2)	7142(1)	8265(1)	20(1)
C(1)	4681(2)	6138(1)	8215(1)	23(1)
C(2)	3398(2)	5731(1)	8327(1)	24(1)
C(3)	2203(2)	5621(1)	9400(1)	21(1)
C(4)	1245(2)	5738(1)	9969(1)	20(1)
C(5)	1342(2)	5341(1)	10564(1)	24(1)
C(6)	466(2)	5374(1)	11133(1)	26(1)
C(7)	-600(2)	5804(1)	11070(1)	23(1)
C(8)	-747(2)	6219(1)	10492(1)	19(1)
C(9)	211(2)	6207(1)	9933(1)	18(1)
C(10)	-1943(2)	6641(1)	10502(1)	20(1)
C(11)	-3454(2)	7462(1)	10200(1)	23(1)
C(12)	-3253(2)	8136(1)	10360(1)	22(1)
C(13)	-2743(2)	8471(1)	9694(1)	25(1)
C(14)	-500(2)	8734(1)	9324(1)	20(1)
C(15)	933(2)	8693(1)	9080(1)	20(1)
C(16)	1679(2)	9236(1)	9068(1)	25(1)
C(17)	3045(2)	9277(1)	8841(1)	27(1)
C(18)	3635(2)	8758(1)	8586(1)	24(1)
C(19)	2954(2)	8199(1)	8587(1)	20(1)
C(20)	1584(2)	8156(1)	8853(1)	17(1)
C(21)	3710(2)	7700(1)	8273(1)	21(1)
C(22)	4243(2)	6739(1)	7842(1)	25(1)
C(23)	5557(3)	5812(1)	7668(1)	32(1)
C(24)	5588(2)	6229(1)	8946(1)	28(1)
C(25)	653(3)	4955(1)	11786(1)	37(1)
C(26)	-2257(2)	8241(1)	11059(1)	29(1)
C(27)	-4747(2)	8383(1)	10477(1)	29(1)
C(28)	3830(3)	9868(1)	8876(2)	42(1)
O(5W)	-1865(2)	8195(1)	7491(1)	33(1)
O(6W)	599(2)	7762(1)	6923(1)	29(1)
O(7W)	-2688(3)	9305(1)	7838(2)	69(1)

Table 3. Anisotropic displacement parameters ($Å^2x10^3$) for $[Ni_2([22]\text{HMTADO})(H_2O)_4](ClO_4)_2 \cdot 3H_2O$

	U^{11}	U^{22}	U^{33}	U^{23}	U^{13}	U^{12}
Ni(1)	17(1)	16(1)	17(1)	-1(1)	3(1)	-1(1)
Ni(2)	16(1)	17(1)	18(1)	0(1)	3(1)	-1(1)
Cl(1)	38(1)	20(1)	25(1)	4(1)	0(1)	1(1)
O(3)	65(2)	51(1)	106(2)	31(1)	32(1)	33(1)
O(4)	75(2)	57(1)	31(1)	6(1)	-15(1)	-27(1)
O(5)	81(2)	41(1)	26(1)	-3(1)	12(1)	-7(1)
O(6)	46(1)	28(1)	65(1)	18(1)	-6(1)	-8(1)
Cl(2)	21(1)	30(1)	23(1)	-1(1)	2(1)	0(1)
O(7)	68(1)	41(1)	39(1)	-14(1)	1(1)	1(1)
O(8)	22(1)	69(1)	58(1)	19(1)	6(1)	-7(1)
O(9)	34(1)	43(1)	37(1)	8(1)	-1(1)	9(1)
O(10)	36(1)	42(1)	25(1)	2(1)	3(1)	-2(1)
O(1W)	20(1)	25(1)	19(1)	-2(1)	2(1)	1(1)
O(2W)	31(1)	23(1)	18(1)	-2(1)	1(1)	-1(1)
O(3W)	22(1)	21(1)	19(1)	-3(1)	1(1)	-2(1)
O(4W)	24(1)	26(1)	22(1)	0(1)	0(1)	-2(1)
O(1)	20(1)	18(1)	17(1)	1(1)	3(1)	-1(1)
O(2)	20(1)	17(1)	21(1)	-1(1)	4(1)	-2(1)
N(1)	18(1)	20(1)	22(1)	-3(1)	2(1)	-2(1)
N(2)	18(1)	20(1)	19(1)	-2(1)	2(1)	-2(1)
N(3)	20(1)	21(1)	20(1)	0(1)	2(1)	1(1)
N(4)	21(1)	23(1)	19(1)	0(1)	5(1)	1(1)
C(1)	22(1)	22(1)	25(1)	-3(1)	7(1)	1(1)
C(2)	24(1)	21(1)	26(1)	-7(1)	5(1)	0(1)
C(3)	18(1)	17(1)	27(1)	-2(1)	1(1)	1(1)
C(4)	19(1)	18(1)	24(1)	0(1)	1(1)	-4(1)
C(5)	22(1)	20(1)	29(1)	3(1)	0(1)	-1(1)
C(6)	26(1)	25(1)	26(1)	6(1)	-1(1)	-5(1)
C(7)	23(1)	26(1)	21(1)	1(1)	4(1)	-6(1)
C(8)	18(1)	20(1)	19(1)	-1(1)	1(1)	-4(1)
C(9)	19(1)	16(1)	17(1)	-1(1)	-1(1)	-6(1)
C(10)	16(1)	24(1)	19(1)	-2(1)	4(1)	-3(1)
C(11)	18(1)	25(1)	28(1)	-1(1)	4(1)	0(1)
C(12)	17(1)	25(1)	25(1)	-2(1)	3(1)	1(1)
C(13)	20(1)	24(1)	31(1)	2(1)	4(1)	5(1)
C(14)	24(1)	18(1)	19(1)	0(1)	1(1)	3(1)
C(15)	23(1)	19(1)	19(1)	2(1)	2(1)	-1(1)
C(16)	32(1)	18(1)	25(1)	0(1)	6(1)	-1(1)
C(17)	32(1)	20(1)	28(1)	3(1)	4(1)	-7(1)
C(18)	23(1)	25(1)	26(1)	5(1)	3(1)	-6(1)
C(19)	21(1)	21(1)	18(1)	2(1)	2(1)	-2(1)
C(20)	20(1)	18(1)	14(1)	1(1)	0(1)	-1(1)
C(21)	20(1)	24(1)	20(1)	5(1)	4(1)	-1(1)
C(22)	27(1)	26(1)	23(1)	-1(1)	10(1)	2(1)
C(23)	32(1)	30(1)	37(1)	-5(1)	15(1)	4(1)
C(24)	22(1)	31(1)	31(1)	-1(1)	3(1)	-2(1)
C(25)	35(1)	41(1)	34(1)	17(1)	3(1)	2(1)
C(26)	24(1)	37(1)	27(1)	-8(1)	2(1)	3(1)
C(27)	21(1)	32(1)	35(1)	-3(1)	7(1)	4(1)
C(28)	45(2)	25(1)	59(2)	0(1)	19(1)	-14(1)
O(5W)	34(1)	33(1)	31(1)	3(1)	-1(1)	6(1)
O(6W)	28(1)	30(1)	28(1)	1(1)	3(1)	-2(1)
O(7W)	61(2)	44(1)	94(2)	-30(1)	-30(1)	11(1)

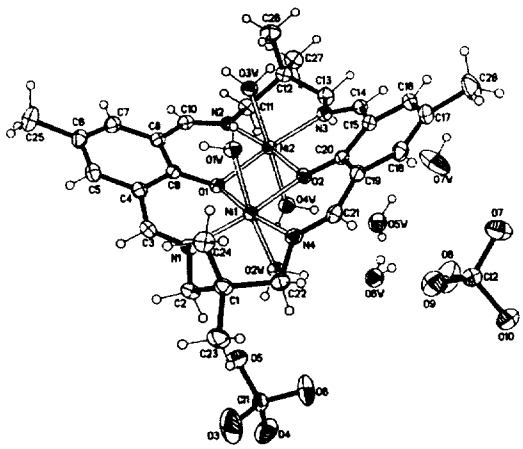

Fig. 1. Structural representation of for the $[Ni_2([22]\text{-}HMTADO)(H_2O)_4](ClO_4)_2 \cdot 3H_2O$ complex.

Table 4. Selected bond lengths (Å) for $[Ni_2([22]\text{-}HMTADO)(H_2O)_4](ClO_4)_2 \cdot 3H_2O$

Ni(1)-N(1)	2.0053(17)	Ni(1)-O(1W)	2.1271(14)
Ni(1)-N(4)	2.0066(17)	Ni(1)-O(2W)	2.1634(14)
Ni(2)-N(2)	1.9944(17)	Ni(2)-O(3W)	2.2253(14)
Ni(2)-N(3)	2.0063(17)	Ni(2)-O(4W)	2.1209(14)
Ni(1)-O(2)	2.0101(14)		
Ni(1)-O(1)	2.0328(14)	Ni(1)-Ni(2)	3.0768(4)
Ni(2)-O(2)	2.0138(14)		
Ni(2)-O(1)	2.0277(14)		

where the nickel(II) ions are coordinated by the two oxygen atoms of water molecules of the nickel basal planes (NiN_2O_4) in trans positions, respectively.

The macrocyclic complex adopts an essentially flat structure with the two octahedral nickel centers bridged by the two phenoxide oxygen atoms, with quite large Ni-O-Ni angles (98.53(6)° and 99.50(6)°). The sum of angles at the phenoxide oxygens is almost exactly 360° (359.66°), indicating no square oxygen distortion. The sum of angles at the nickel basal planes (NiN_2O_4) is almost exactly 360° (359.96° and 359.80°), indicating no plane distortion.

The nickel centers are separated by 3.0768(4) Å and in plane nickel-ligand distances fall in the range 1.9944(17)-2.0328(14) Å. An angle of 21.07° exists between the benzene mean planes of macrocycle and the nickel basal planes. This is bent owing to

Table 5. Selected angles [°] for $[Ni_2([22]\text{-}HMTADO)(H_2O)_4](ClO_4)_2 \cdot 3H_2O$

N(1)-Ni(1)-N(4)	97.05(7)
N(1)-Ni(1)-O(2)	171.19(6)
N(4)-Ni(1)-O(2)	91.58(6)
N(1)-Ni(1)-O(1)	90.53(6)
N(4)-Ni(1)-O(1)	172.23(6)
O(2)-Ni(1)-O(1)	80.80(6)
N(1)-Ni(1)-O(1W)	91.97(6)
N(4)-Ni(1)-O(1W)	89.30(6)
O(2)-Ni(1)-O(1W)	86.38(6)
O(1)-Ni(1)-O(1W)	88.71(5)
N(1)-Ni(1)-O(2W)	96.06(6)
N(4)-Ni(1)-O(2W)	91.31(6)
O(2)-Ni(1)-O(2W)	85.44(6)
O(1)-Ni(1)-O(2W)	89.59(6)
O(1W)-Ni(1)-O(2W)	171.81(6)
N(1)-Ni(1)-Ni(2)	131.09(5)
N(4)-Ni(1)-Ni(2)	131.63(5)
O(2)-Ni(1)-Ni(2)	40.17(4)
O(1)-Ni(1)-Ni(2)	40.67(4)
O(1W)-Ni(1)-Ni(2)	85.23(4)
O(2W)-Ni(1)-Ni(2)	88.26(4)
N(2)-Ni(2)-N(3)	96.81(7)
N(2)-Ni(2)-O(2)	171.07(6)
N(3)-Ni(2)-O(2)	91.75(6)
N(2)-Ni(2)-O(1)	90.62(6)
N(3)-Ni(2)-O(1)	172.57(6)
O(2)-Ni(2)-O(1)	80.83(6)
N(2)-Ni(2)-O(4W)	95.10(6)
N(3)-Ni(2)-O(4W)	93.08(6)
O(2)-Ni(2)-O(4W)	86.95(6)
O(1)-Ni(2)-O(4W)	86.19(6)
N(2)-Ni(2)-O(3W)	90.64(6)
N(3)-Ni(2)-O(3W)	90.85(6)
O(2)-Ni(2)-O(3W)	86.67(6)
O(1)-Ni(2)-O(3W)	89.11(5)
O(4W)-Ni(2)-O(3W)	172.61(6)
N(2)-Ni(2)-Ni(1)	131.23(5)
N(3)-Ni(2)-Ni(1)	131.80(5)
O(2)-Ni(2)-Ni(1)	40.08(4)
O(1)-Ni(2)-Ni(1)	40.80(4)
O(4W)-Ni(2)-Ni(1)	87.63(4)
O(3W)-Ni(2)-Ni(1)	85.68(4)

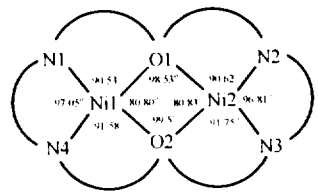

the chair conformation effect of the six-membered ring with trimethylene chain linking the azomethine nitrogen donors and nickel.

The two methyl groups (C(24) and C(26)) attached to the trimetylenes are situated eclipsed conformation. Four water molecules occupy axial positions in a trans arrangement with somewhat longer contacts [Ni(1)-O(1W) : 2.1271(14) Å, Ni(1)-O(2W) : 2.1634(14) Å, Ni(2)-O(3W) : 2.2253(14) Å, Ni(2)-O(4W) : 2.1209(14) Å]. The angles O_{axial}-Ni-O_{axial} [O(1W)-Ni(1)-O(2W) : 171.81(6), O(3W)-Ni(2)-O(4W) : 172.61(6)] are smaller than the ideal value of 180° by hydrogen bonding between coordinated water, indicating that the donor atoms are not able to achieve the axial positions of a perfect octahedron.

In general, hydrogen bonding plays a principal role in the packing of the title compound. There are five types of H-bonds : between coordinated waters, coordinated water - lattice water, coordinated water - perchlorate ion, lattice water - perchlorate ion, and between lattice waters (Table 6). These

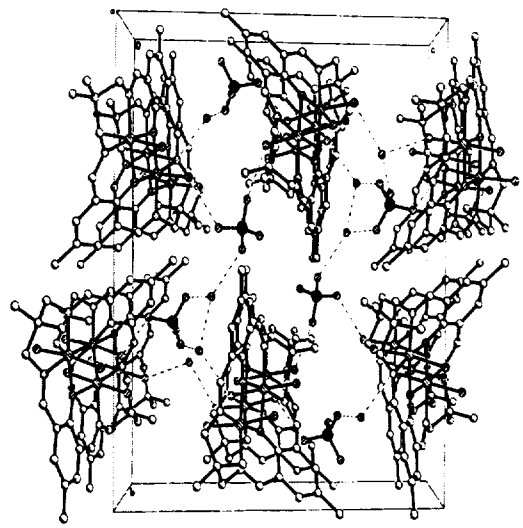

Fig. 2. The molecular packing diagram of $[[Ni_2([22]\text{-HMTADO})(H_2O)_4](ClO_4)_2 \cdot 3H_2O$. The hydrogen bonds are indicated by dotted lines.

interactions result in a formation of polymeric chains (Fig. 2). This chain forms a related layer structure, but within the layers dinuclear cation $[Ni_2([22]\text{-HMTADO})(H_2O)_4]^{2+}$ ions arrange zig-zag

Table 6. Selected bond lengths (Å) and angles(°) for hydrogen bond of $[Ni_2([22]\text{-HMTADO})(H_2O)_4]ClO_4 \cdot 3H_2O$

D-H···A	d(D-H)	d(H···A)	⟨DHA	d(D···A)
between coordinated waters				
O1W-H1WA···O3W	0.834	1.930	161.54	2.734
O4W-H4WB···O2W	0.834	2.145	151.39	2.905
coordinated water - lattice water				
O2W-H2WB···O6W	0.839	2.006	164.78	2.824
O3W-H3WA···O6W [x, -y+3/2, z+1/2]	0.839	1.970	167.72	2.795
O4W-H4WA···O5W	0.836	1.932	174.62	2.765
coordinated water - ClO_4				
O1W-H1WB···O10 [x, -y+3/2, z+1/2]	0.838	2.060	170.58	2.889
O2W-H2WA···O5	0.836	1.976	175.03	2.810
O3W-H3WB···O6 [x, -y+3/2, z+1/2]	0.841	1.953	166.36	2.777
lattice water - ClO_4				
O5W-H5WA···O9 [x-1, y, z]	0.838	2.043	157.32	2.834
O6W-H6WB···O8	0.791	2.151	151.69	2.872
O7W-H7WA···O3 [-x, y+1/2, -z+3/2]	0.838	1.981	173.29	2.815
O7W-H7WB···O7 [x-1, y, z]	0.834	2.115	161.23	2.918
between lattice waters				
O5W-H5WB···O7W	0.840	1.903	154.40	2.685
O6W-H6WA···O5W	0.852	1.965	165.13	2.797

configurations.

2. Electronic absorption spectrum

The pale green crystals of complex (1) become pale yellow-green in water. The electronic absorption spectrum of this solution is typical of six-coordinate nickel(II) complex indicating that species existing in solution is $[Ni_2([22]\text{-HMTADO})(H_2O)_4]^{2+}$. The complex ion in aqueous solution at room temperature is represented in Fig. 3.

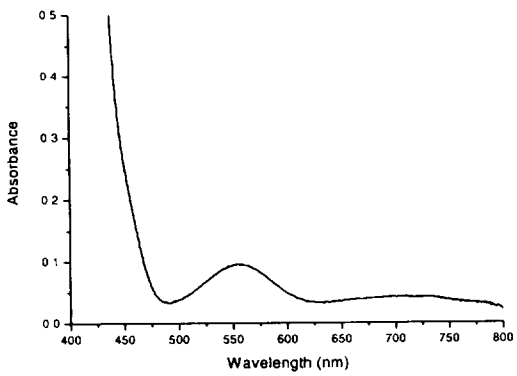

Fig. 3. The electronic absorption spectrum of $[Ni_2([22]\text{-HMTADO})(H_2O)_4]^{2+}$ in aqueous solution at 298 K(concentration : 5.0×10^{-3} M).

Much weaker bands are found at lower energy, associated with *d-d* transitions. However, strong absorptions at 300 - 450 nm are clearly associated with charge transfer transitions, which reflect the presence of highly delocalized π marcrocyclic framework. Two *d-d* bands observed for the complex at 13.717 cm^{-1} (ε = 8.4 $dm^3mol^{-1}cm^{-1}$), 18.051 cm^{-1} (ε = 19.2 $dm^3mol^{-1}cm^{-1}$) can be attributed in an octahedral model to the transition. The ground state of d^8 in an octahedral coordination is $^3A_{2g}$. Thus, these bands may be assigned to the spin allowed transitions $^3A_{2g} \rightarrow {}^3T_{2g}(F)$ and $^3A_{2g} \rightarrow {}^3T_{1g}(F)$, respectively. $^3A_{2g} \rightarrow {}^3T_{1g}(P)$ transition is not separated by the transfer effect to visible range of charge transfer transitions and absorptions of marcrocycle ligand.

3. Infrared spectra

The infrared spectra of (1) and (2) recorded at room temperature are presented in Fig. 4 and 5. Infrared spectra of both (1) and (2) show ν(C=N) stretching vibration bands in the range ~1630 cm^{-1} and the absence of any carbonyl bands associated with the diformyl-phenol starting materials or nonmarcrocyclic intermediates. The IR spectra displayed C-H stretching vibrations from 3000 to 2800 cm^{-1}. The present complexes exhibited three C-H deformation bands at 1440, 1390, and 1370 cm^{-1} region and two out-of-plan vibration bands 820 and 765 cm^{-1} region.

A strong ionic ClO_4^- band at near 1095 cm^{-1} and 625 cm^{-1} in (2) complex.

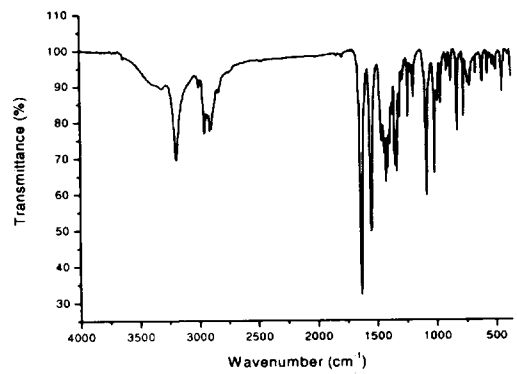

Fig. 4. IR spectrum of $[Ni_2([22]\text{-HMTADO})]Cl_2 \cdot 3H_2O$.

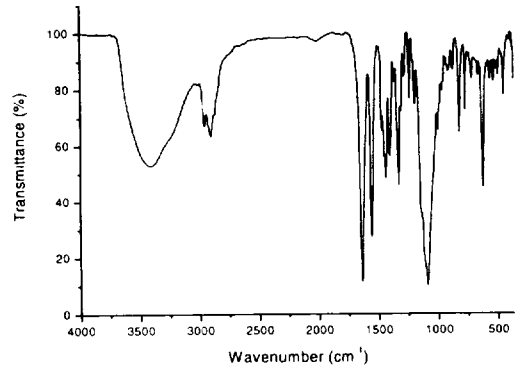

Fig. 5. IR spectrum of $[Ni_2([22]\text{-HMTADO})](ClO_4)_2 \cdot 3H_2O$

4. FAB mass spectra

The FAB mass spectra consist of peaks due to the molecular ions. The molecular ions undergo fragmentation to give species such as $[Ni_2([22]\text{-}HMTADO)]^+$. In the FAB mass spectra of 1 and 2, there is a peak at m/z 575 corresponding to the molecular ions (Fig. 5). These major peaks are associated with peaks of mass one or two greater or less, which are attributed to protonated/deprotonated forms. This also accounts for the slight ambiguities in making assignments. In the mass spectrum of these complexes the peaks observed at m/z 518 are due to fragments $[Ni([22]\text{-}HMTADO)]^+$. In the 1 complex, there are two strong peaks at m/z 610.7 and 648.8, which may be assigned to $[Ni_2([22]\text{-}HMTADO)(Cl)\text{-}H]^+$ and $[Ni_2([22]\text{-}HMTADO)(Cl)_2 + 2H]^+$, respectively. In the 2 complex, there are fairly strong peak at m/z 675.6, which may be assigned to $[Ni_2([22]\text{-}HMTADO)(ClO_4)]^+$.

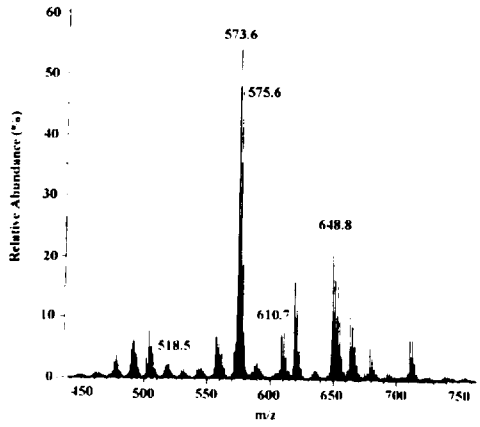

Fig. 6. FAB-mass spectrum of $[Ni_2([22]\text{-}HMTADO)]Cl_2 \cdot 3H_2O$.

5. Thermal stability

Thermogravimetry analysis have been carried out simultaneously for the $[Ni_2([22]\text{-}HMTADO)](ClO_4)_2 \cdot 3H_2O$ complexe (Fig. 8).

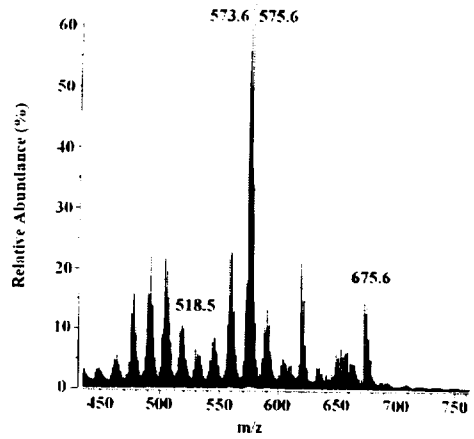

Fig. 7. FAB-mass spectrum of $[Ni_2([22]\text{-}HMTADO)](ClO_4)_2 \cdot 3H_2O$

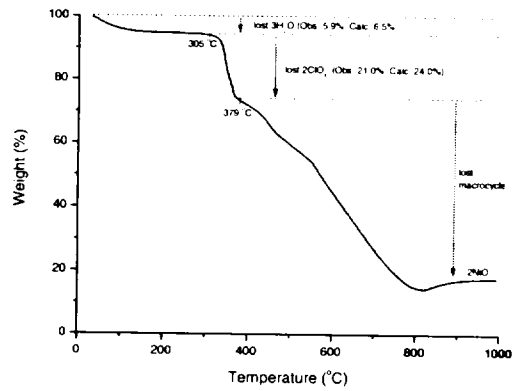

Fig. 8. TGA curve of $[Ni_2([22]\text{-}HMTADO)](ClO_4)_2 \cdot 3H_2O$.

The result indicate that the coordinated macrocycle has relatively high thermal stability. Lattice water is removed at the temperature range ~200℃. Counter ions are lost in the 300~380℃ range. The macrocyclic entity remains unchanged up to 380℃. Finally, the complex is changed to NiO above 800℃.

Reference

1. T. Thomas and T. Thomas. *J. Cell. Mol. Life Sci.* 2001, 58, 244.
2. L. J. Marton and A. E. Pegg. *Annu. Rev. Pharmacol. Toxicol.* 1995, 35, 55.

3. J. W. Sibert. A. H. Cory. and J. G. Cory. *J. Chem. Soc.. Chem. Commun* 2002. 154.
4. L. Messori. F. Abbate. G. Marcon. P. Orioli. M. Fontani. E. Mini. T. Mazzei. S. Carotti. T. O' Connel. and P. Zanello. *J. Med. Chem.* 2000. 43. 3541.
5. D. Kong. L. Meng. J. Ding. Y. Xie. and X. Huang. *Polyhedron* 2000. 19. 217.
6. D. Kong. L. Meng. L. Song. and Y. Xie. *Trans. Metal Chem.* 1999. 24. 553.
7. E. De Clercq. *Biochim. Biophys. Acta* 2002. 1587. 258
8. E. Kikuta. S. Aoki. and E. Kimura. *J. Am. Chem. Soc.* 2001. 123. 7911
9. E. Kimura. I. Nakamura. T. Koike. M. Shionoya. Y. Kodama. T. Ikeda. and M. Shiro. *J. Am. Chem. Soc.* 1994. 116. 4764
10. J. H. Kim. *Chem. Lett.* 2000. 156.
11. E. L. Hegg. S. H. Mortimore. C. L. Cheung. J. E. Huyett. D. R. Powell. and J. N. Burstyn. *Inorg. Chem.* 1999. 38. 2961.
12. K. A. Deal. A. C. Hengge. and J. N. Burstyn. *J. Am. Chem. Soc.* 1996. 118. 1713.
13. K. A. Deal and J. N. Burstyn. *Inorg. Chem.* 1996. 35. 2792.
14. W. H. Jr. Chapman.. and R. Breslow. *J. Am. Chem. Soc.* 1995. 117. 5462.
15. P. Rossi. F. Felluga. P. Tecilla. F. Formaggio. M. Crisma. C. Toniolo. and P. Scrimin. *J. Am. Chem. Soc.* 1999. 121. 6948.
16. E. L. Hegg. K. A.Deal. L. L.Kiessling. and J. N. Burstyn. *Inorg. Chem.* 1997. 36. 1715.
17. C. Sissi. P. Rossi. F. Felluga. F. Formaggio. M. Palumbo. P. Tecilla. C. Toniolo. P. Scrimin. *J. Am. Chem. Soc.* 2001. 123. 6948.
18. E. L. Hegg and J. N. Burstyn. *Inorg. Chem.* 1996. 35. 7474.
19. E. L. Hegg and J. N. Burstyn. *J. Am. Chem. Soc.* 1995. 117. 7015.
20. F. Liang. C. Wu. H. Lin. T. Li. D. Gao. Z. Li. J. Wei. C. Zheng. M. Sun. *Bioorg. Med. Chem. Lett.* 2003. 13. 2469.
21. F. Liang. P. Wang. X. Zhou. T. Li. Z. Li. H. Lin. D. Gao. C. Zhengc. and C. Wu. *Bioorg. Med. Chem. Lett.* 2004. 14. 1901.
22. R. Robson. *Aust. J. Chem.* 1970. 23. 2217.
23. O. Kahn. *Structure and Bonding(Berlin)* 1987. 68. 89.
24. D. E. Feenton. H. Okawa. *Prespectives on Bioinorg. Chem.* 1993. 2. 81.
25. N. Strater. T. Klabunde. P. Tucker. H. Witzel. and B. Krebs. *Science* 1995. 268. 1489.
26. C. R. Kissinger. H. E. Parge. D. R. Knighton. C. T. Lewis. L. A. Pelletier. A. Tempczyk. V. J. Kalish. K. D. Tecker. R. E. Shiwalter. E. W. Moomaw. L. N. Gastinel. N. Habuka. X. Chen. F. Maldonado. J. E. Barker. R. Bacquet. and J. E. Villafranca. *Nature* 1995. 378. 641.
27. M. P. Egloff. P. T. W. Cohen. P. Reinemer. and D. Barford. *J. Mol. Biol.* 1995. 254. 942.
28. D. E. Fenton and H. Ōkawa. *Chem. Ber./ Recueil* 1997. 130. 433.
29. U. Casellato. P. A. Vigato. and M. Vidali. *Coord. Chem. Rev.* 1977. 23. 31.
30. D. E. Fenton. U. Casellato. P. A. Vigato. and M. Vidali. *Inorg. Chim. Acta* 1982. 62. 57.
31. S. F. Groh and Israel *J. Chem.* 1976/77. 15. 277.
32. P. Zanello. S. Tanburini. P. L. Vigato. and G. A. Mazzocchin. *Coord. Chem. Rev.* 1987. 77. 165.
33. A. J. Edwards. B. F. Hoskins. E. H. Kachab. A. Markiewicz. K. S. Murray. and R. Robson. *Inorg. Chem* 1992. 31. 3584.
34. B. F. Hoskins. R. Robson. and P. J. Smith. *J. Chem. Soc.. Chem. Commun.* 1990. 488.
35. V. McKee and S. S. Tandon. *J. Chem. Soc.. Dalton Trans.* 1991. 221.
36. S. S. Tandon. L. K. Thompson. and J. N. Beidson. *J. Chem. Soc.. Chem. Commun.* 1992. 911.
37. D. D. Perrin and W. L. F. Armarego. *Purification of Laboratory Chemicals. Pergamon.* 3rd edn.. 1988.

38. T. Shozo. *Bull. Chem. Soc. Jpn.* 1984. 57. 2683.
39. J. C. Byun. Y. C. Park. and C. H. Han. *J. Kor. Chem. Soc.* 1999. 43/3. 267.
40. Bruker. *SAINTPLUS NT Version 5.0. Software Reference Manual Bruker AXS: Madison.* Wisconsin. 1998.
41. Bruker. *SHELXTL NT Version 5.16. Program for Solution and Refinement of Crystal Structures Bruker AXS*: Madison. Wisconsin. 1998.